

# PAHs contribution to the infrared output energy of the Universe at $z \simeq 2$

G. Lagache<sup>1</sup>, H. Dole<sup>1,2</sup>, J.-L. Puget<sup>1</sup>, P. G. Pérez-González<sup>2</sup>, E. Le Floc'h<sup>2</sup>, G. H. Rieke<sup>2</sup>, C. Papovich<sup>2</sup>, E. Egami<sup>2</sup>, A. Alonso-Herrero<sup>2</sup>, C. W. Engelbracht<sup>2</sup>, K.D. Gordon<sup>2</sup>, K. A. Misselt<sup>2</sup>, and J. E. Morrisson<sup>2</sup>

## ABSTRACT

We present an updated phenomenological galaxy evolution model to fit the *Spitzer* 24, 70 and 160  $\mu\text{m}$  number counts as well as all the previous mid and far infrared observations. Only a minor change of the co-moving luminosity density distribution in the previous model (Lagache, Dole, Puget 2003), combined with a slight modification of the starburst template spectra mainly between 12 and 30  $\mu\text{m}$ , are required to fit all the data available. We show that the peak in the MIPS 24  $\mu\text{m}$  counts is dominated by galaxies with redshift between 1 and 2, with a non negligible contribution from the  $z \geq 2$  galaxies ( $\sim 30\%$  at  $S=0.2$  mJy). The very close agreement between the model and number counts at 15 and 24  $\mu\text{m}$  strikingly implies that (1) the PAHs (Polycyclic Aromatic Hydrocarbons) features remain prominent in the redshift band 0.5 to 2.5 and (2) the IR energy output has to be dominated by  $\sim 3 \cdot 10^{11} L_{\odot}$  to  $\sim 3 \cdot 10^{12} L_{\odot}$  galaxies from redshift 0.5 to 2.5. Combining *Spitzer* with the *Infrared Space Observatory (ISO)* deep cosmological surveys gives for the first time an unbiased view of the infrared Universe from  $z=0$  to  $z=2.5$ .

*Subject headings:* infrared: galaxies – galaxies: evolution – galaxies: model

## 1. Introduction

A Cosmic far-Infrared Background (CIB) that would trace the peak of the star-formation and metal production in galaxy assembly has long been predicted. The first observational evidence for such a background was reported by Puget et al. (1996) (see Hauser & Dwek 2001, for a review). This discovery, together with recent cosmological surveys in the infrared

---

<sup>1</sup>Institut d’Astrophysique Spatiale, bât 121, Université Paris-Sud, F-91405 Orsay Cedex

<sup>2</sup>Steward Observatory, University of Arizona, 933 N Cherry Ave, Tucson, AZ 85721, USA

(IR) and submillimeter, has opened new perspectives on our understanding of galaxy formation and evolution. The surprisingly large amount of energy in the CIB shows that it is crucial to probe the galaxies contributing to it to understand when and how the bulk of stars formed in the Universe.

To understand the sources contributing to the CIB and to interpret the deep source counts, we have developed a phenomenological model that constrains in a simple way the IR luminosity function evolution with redshift, and fits all the existing source counts consistent with the redshift distribution, the CIB intensity, and, for the first time, the CIB fluctuation observations from the mid-IR to the submm range (Lagache et al. 2003). *Spitzer* has provided deep new multiwavelength source counts from 24 to 160  $\mu\text{m}$  (Papovich et al. 2004, Dole et al. 2004a). We use these new data to search for a new optimisation of the Lagache et al. (2003) model parameters. A remarkable result is that only a minor change of the co-moving luminosity density distribution combined with a slight modification of the starburst model spectra, mainly for the  $12 \leq \lambda \leq 30 \mu\text{m}$  range, are required to fit all the previous data together with the new constraints.

## 2. The model

The model is discussed extensively in Lagache et al. (2003). Our goal is to build the simplest model with the fewest free parameters and separate ingredients. We fix the cosmology to  $\Omega_\Lambda=0.7$ ,  $\Omega_0=0.3$  and  $h=0.65$ . We assume that IR galaxies are mostly powered by star formation and hence we use Spectral Energy Distributions (SEDs) typical of star-forming galaxies<sup>3</sup>. Although some of the galaxies will have AGN-dominated SEDs, they are a small enough fraction ( $< 10\%$ : Alonso Herrero et al. 2004) that they do not affect the results significantly. We therefore construct 'normal' and starburst galaxy template SEDs: a single form of SED is associated with each activity type and luminosity. We assume that the Luminosity Function (LF) is represented by these two activity types and that they evolve independently. We search for the form of evolution that best reproduces the existing data. The new optimisation of the model parameters reproduces: (i) the number counts at 15, 24, 60, 70, 90, 160, 170, and 850  $\mu\text{m}$ , (ii) the known redshift distributions (mainly at 15 and 170  $\mu\text{m}$ ), (iii) the local luminosity functions at 60 and 850  $\mu\text{m}$ , (iv) the CIB (from 100 to 1000  $\mu\text{m}$ ) and its fluctuations (at 60, 100 and 170  $\mu\text{m}$ ).

Compared with the form of the model derived by Lagache et al. (2003), only a slight change

---

<sup>3</sup>This assumption is based primarily on observations by ISOCAM and ISOPHOT, but is confirmed by the first *Spitzer* studies of galaxy SEDs in the Lockman Hole and Groth Strip (Le Floch et al. 2004; Alonso Herrero et al. 2004)

of the co-moving luminosity density distribution is required (Fig. 1), together with minor modifications to the starburst template spectra mainly between 12 and 30  $\mu\text{m}$  (Fig. 2). The modified starburst spectra still reproduce the color diagrams of Soifer & Neugebauer 1991 (12/25 versus 60/100). We do not modify any other parameters in the model, nor the SED of the 'normal' galaxy template nor the SED of the starburst galaxy templates at longer wavelengths, nor the parametrisation of the local LF.

PAHs radiate about 10% of the 1-1000  $\mu\text{m}$  luminosity in a set of features concentrated mostly between 6 and 15  $\mu\text{m}$  (Fig. 2). This set of features is the strongest spectral concentration known in galaxy spectra. The features affect strongly the mid-IR number counts when the redshift brings them into the bandpass filter. For the 15  $\mu\text{m}$  ISOCAM observations, the peak contribution arises when the 7.7  $\mu\text{m}$  maximum is close to the middle of the band i.e.  $z \sim 0.8$ . The ISOCAM 15  $\mu\text{m}$  counts showed the existence of a maximum in the redshift distribution just at that redshift. Furthermore, it leads to a maximum in the counts (normalised to the Euclidian, e.g. on Fig. 3), which can exist only when the IR energy output in the critical redshift range is dominated by a well defined luminosity range. Our model predicted a similar behaviour for the 24  $\mu\text{m}$  band.

### 3. Results

#### 3.1. Source counts

We show the comparison of the number counts at 15, 60, 170 and 850  $\mu\text{m}$  with the observations and as well as the new *Spitzer* 24  $\mu\text{m}$  (Papovich et al. 2004), 70 and 160  $\mu\text{m}$  (Dole et al. 2004a) counts in Fig. 3 and Fig. 4. The updated model reproduces very well the counts at 15 and 24  $\mu\text{m}$  without any significant changes in the other number counts, as well as the CIB and its fluctuations and the redshift distributions of resolved sources at 15, 60, 170 and 850  $\mu\text{m}$ . The agreement between the observed counts and the model at 24  $\mu\text{m}$  is excellent.

#### 3.2. First interpretation of the *Spitzer*/*MIPS* results

The consistency of the model from the mid-IR and far-IR to the submm indicates that the underlying assumptions are valid up to redshift 2.5. In particular, the very close agreement between the model and number counts at 15 and 24  $\mu\text{m}$  implies that the PAH features remain prominent in the redshift range 0.5 to 2.5. Furthermore, the well-defined

bump in the 24  $\mu\text{m}$  number counts (normalised to the Euclidian) at  $S \simeq 0.3$  mJy (Fig. 4) implies at  $z \simeq 2$  that  $L_{8\mu\text{m}} = 3.2 \cdot 10^{11} L_{\odot}$  which corresponds to  $L_{1-1000\mu\text{m}} = 3.5 \cdot 10^{12} L_{\odot}$ . These luminosities have to dominate the IR energy output at that redshift (as shown on Fig. 7). As a comparison, an IR energy output dominated by  $L_{\star}$  galaxies at  $z \simeq 2$  would maximise the 24  $\mu\text{m}$  counts around 3  $\mu\text{Jy}$  which is totally inconsistent with the observation since most of the CIB at 24  $\mu\text{m}$  is resolved at flux densities brighter than  $\sim 60$   $\mu\text{Jy}$ .

Using the new model of IR galaxy evolution, Dole et al. (2004b) have made new determinations of the confusion limits for MIPS (Multi Band Imaging Photometer for *Spitzer*). A summary is provided in Table 1. Fig. 5 shows the updated redshift distributions for such confusion-limited surveys. At 24  $\mu\text{m}$ , the deepest surveys will probe star formation up to redshift 3. In the far-IR, MIPS surveys will probe the largely unexplored window  $1 \leq z \leq 2$ . In Fig 6, we show the different redshift contributions to the 24  $\mu\text{m}$  number counts. The peak in the counts is dominated by galaxies with redshift between 1 and 2. There is also a non negligible contribution from  $z > 2$  galaxies (30% at  $S = 0.2$  mJy). The integral of the source counts down to 60  $\mu\text{Jy}$  gives  $1.9 \text{ nW m}^{-2} \text{ sr}^{-1}$ , in excellent agreement with Papovich et al. (2004). It represents about 63% of the CIB at 24  $\mu\text{m}$ . It should also be noted from Fig. 6 that the redshift distribution changes sharply for fluxes between 0.3 and 2 mJy. For sources weaker than 150  $\mu\text{Jy}$ , the redshift distribution remains about constant.

#### 4. Conclusion

We have updated the model of Lagache et al. (2003) to fit the new constraints from *Spitzer* data. We show that only a small change of the co-moving luminosity density distribution and of the starburst template spectra are required to fit all the observations from the mid-IR to the sub-millimeter. The agreement between the model and all the data demonstrates that the integrated SEDs from galaxies still have prominent 6-9  $\mu\text{m}$  emission from PAH features up to redshift 2.5. It clearly shows that the population of IR galaxies is not dominated by galaxies with featureless continuum spectra (such as AGN-type SEDs in the mid-IR). The fraction of the energy radiated by the PAHs is about one tenth of the total IR radiation locally and remains roughly constant between redshifts 0.5 and 2.5.

Our initial model predicted that the IR output energy had to be dominated by galaxies with luminosities increasing rapidly with redshift ( $L_{1-1000\mu\text{m}} \simeq 3 \cdot 10^{12} L_{\odot}$  at  $z = 2.5$ ). This was needed mainly to account for the SCUBA counts (the total energy output at that redshift being mostly driven by the submillimeter extragalactic background level). The excellent agreement between the 24  $\mu\text{m}$  counts and the model confirms strikingly the evolution of the IR luminosity function as being dominated in energy by  $\sim 3 \cdot 10^{11} L_{\odot}$  to  $\sim 3 \cdot 10^{12} L_{\odot}$  galaxies

from redshift 0.5 to 2.5.

We have for the first time with *Spitzer* an unbiased view of the IR Universe up to redshift 2.5. With all the mid-IR to sub-mm data, the model is now very well constrained up to  $z \simeq 2.5$ . Other predictions, together with the number counts of all the planned and future mid-IR to mm surveys, will be available on the web page:  
[http://www.ias.fr/PPERSONO/glagache/act/gal\\_model.html](http://www.ias.fr/PPERSONO/glagache/act/gal_model.html).

This work is based on observations made with the *Spitzer* Space Telescope, which is operated by the Jet Propulsion Laboratory, California Institute of Technology under NASA contract 1407. We thank the funding from the MIPS project, which is supported by NASA through the Jet Propulsion Laboratory, subcontract #960785. GL warmly thanks the MIPS IT in Tucson, HD and JLP for this fruitful collaboration and G.H.R for his careful reading of the manuscript.

## REFERENCES

- Alonso Herrero et al., 2004, this issue
- Barger A.J., Cowie L.L., Sanders D.B., 1999, ApJ 518, L5
- Bertin E., Dennefeld M., Moshir M., 1997, A&A 323, 685
- Blain A.W., Kneib J.-P., Ivison R.J. et al., 1999, ApJ 512, L87
- Borys C., Chapman S., Halpern M. et al., 2003, MNRAS, 344, 385
- Dole H., Gispert R., Lagache G. et al., 2001, A&A 372, 364
- Dole H., Lagache G., Puget J.-L., 2003, ApJ, 585, 617
- Dole H., Le Floc'h E., Papovich C. et al., 2004a, ApJ, this issue
- Dole H., Rieke G.H., Lagache G. et al., 2004b, ApJ, this issue
- Lagache G., Dole H., Puget J.-L., 2003, MNRAS 338, 555
- Elbaz D., Cesarsky C.J., Fadda D. et al., 1999, A&A 351, 37
- Gispert R., Lagache G., Puget J.-L., 2000, A&A 360, 1
- Gregorich D.T., Neugebauer G., Soifer B.T., Gunn J.E., Herter T.L., 1995, AJ 110, 259

- Hauser M.G., Dwek E., 2001, ARAA, 37, 249
- Hacking P.B., Houck J.R., 1987, ApJS 63, 311
- Hughes D.H., Dunlop J.S., Rowan-Robinson M. et al., 1998, Nature 394, 241
- Le Floc’h E., et al., 2004, ApJ, this issue
- Lonsdale C.J., Hacking P.B., Conrow T.B., Rowan-Robinson M., 1990, ApJ 358, 20
- Puget J.-L., Abergel A., Bernard J.-P. et al., 1996, A&A 308, L5
- Papovich C., Dole H., Egami E., 2004, ApJ, this issue
- Rowan-Robinson M., Saunders W., Lawrence A., Leech K., 1991, MNRAS 253, 485
- Saunders W., Rowan-Robinson M., Lawrence A. et al. 1990, MNRAS 242, 318
- Scott S.E., Fox M.J., Dunlop J.S. et al., 2002, MNRAS 331, 817
- Soifer B.T., Neugebauer G., 1991, AJ 101, 354
- Smail I., Ivison R.J., Blain A.W., 1997, ApJ 490, L5
- Webb T.M.A., Eales S.A., Lilly S.J. et al., 2003, ApJ, 587, 41

Table 1.  $1 \sigma_c$  confusion noise values using the best confusion estimator of Dole et al. (2003), confusion limit  $S_{lim}$  and the value of  $q = S_{lim}/\sigma_c$

	24 $\mu\text{m}$	70 $\mu\text{m}$	160 $\mu\text{m}$
$1 \sigma_c$	8.0 $\mu\text{Jy}$	0.47 mJy	10.6 mJy
$S_{lim}$	<b>56 <math>\mu\text{Jy}</math></b>	<b>3.2 mJy</b>	<b>39.8 mJy</b>
q	7.0	6.8	3.8

<sup>a</sup>Using the source density criterion

<sup>b</sup>In this case, the photometric and source density criteria agree

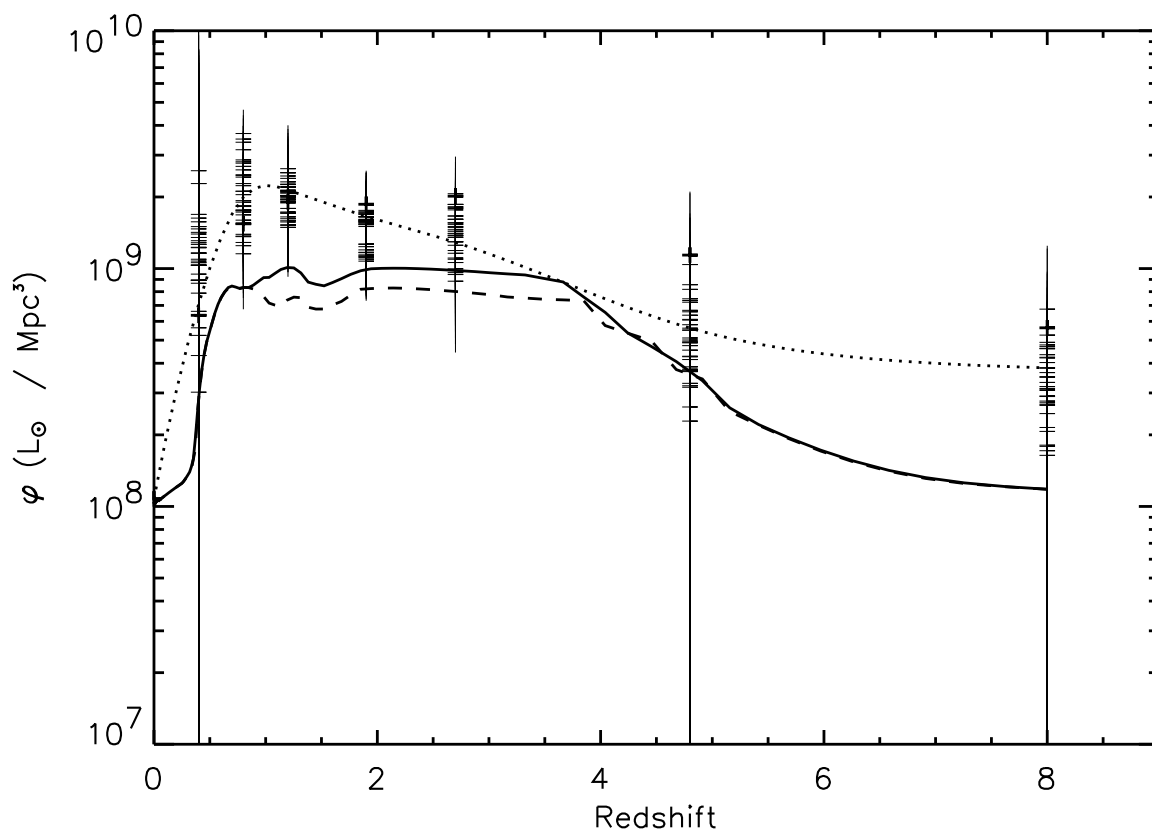


Fig. 1.— Co-moving luminosity density distribution of the Lagache et al. (2003) model (dashed line) and the updated model presented here (continuous line). Also shown for comparison is the co-moving luminosity density distribution from all cases of Gispert et al. 2001 (crosses with error bars), together with the best fit passing through all cases (dot line).

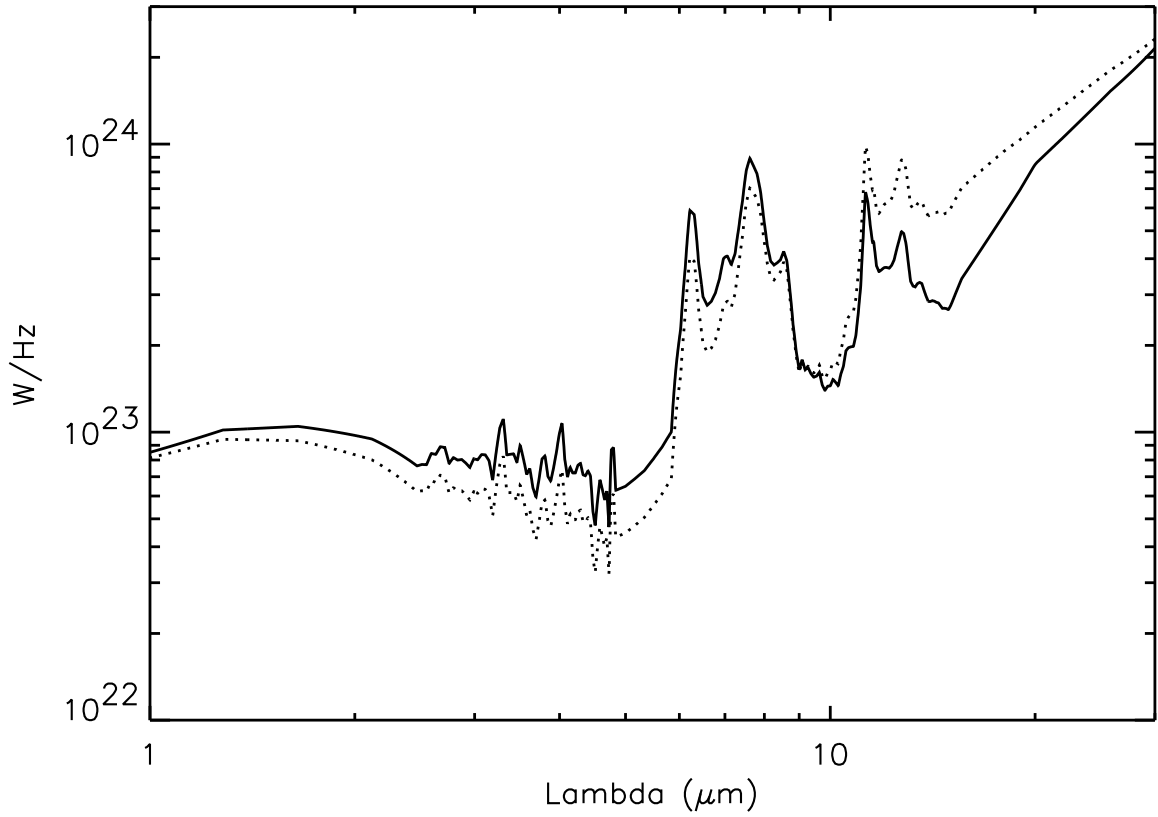


Fig. 2.— Starburst model spectrum for  $L = 3 \cdot 10^{11} L_{\odot}$ . Dashed line: Lagache et al. (2003), continuous line: the present updated version of the model. The spectrum has not been modified for  $\lambda \geq 30 \mu\text{m}$ . The biggest change is about a factor 2 (for a  $3 \cdot 10^{11} L_{\odot}$  galaxy) around  $15 \mu\text{m}$ .

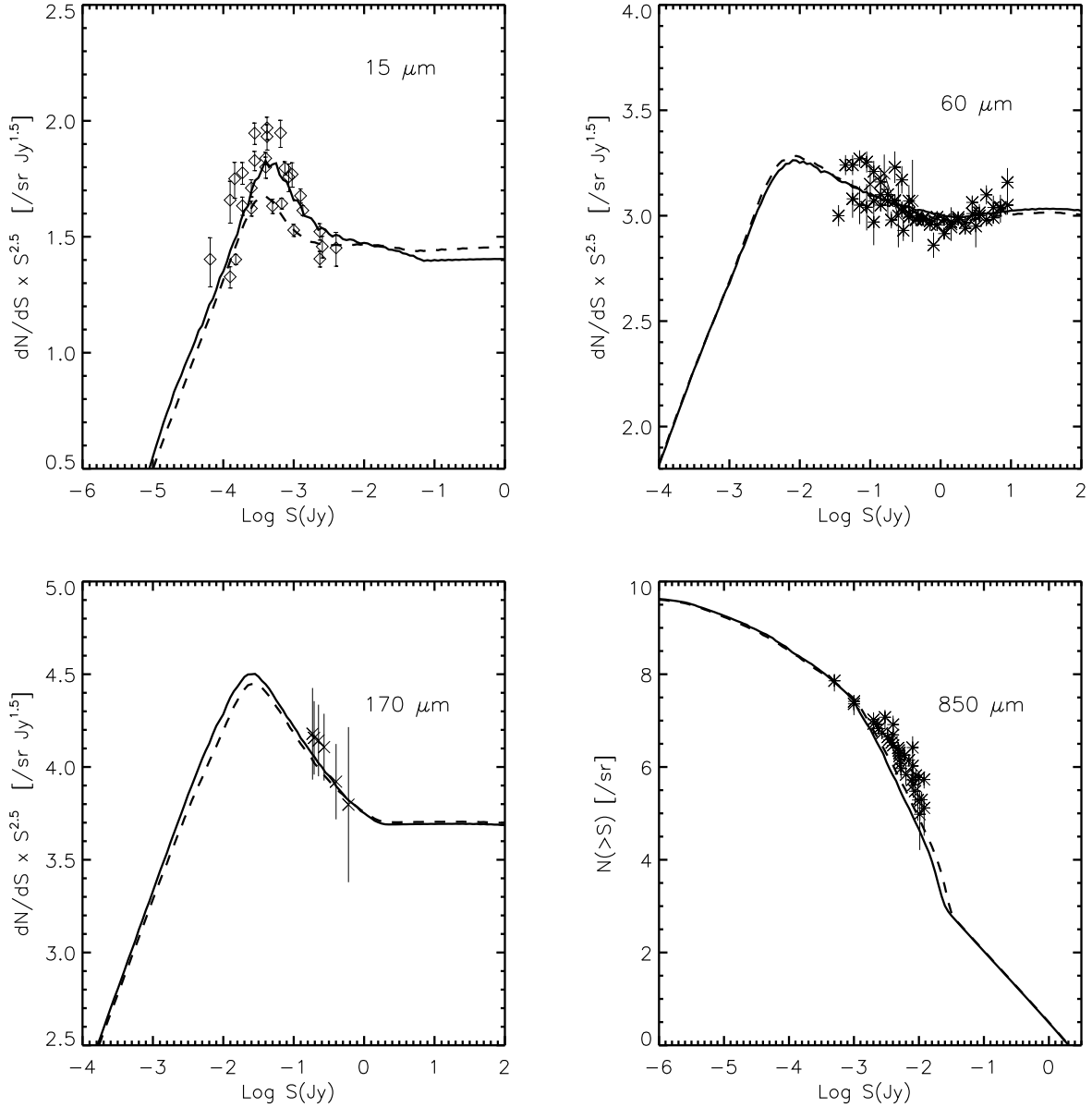


Fig. 3.— Number counts at 15, 60, 170 and 850  $\mu\text{m}$  (in Log) together with the model predictions (present work: continuous line, Lagache et al. 2003: dashed line). Data at 15  $\mu\text{m}$  are from Elbaz et al. (1999), at 170  $\mu\text{m}$  from Dole et al. (2001), at 60  $\mu\text{m}$  from Hacking & Houck (1987), Gregorich et al. (1995), Bertin et al. (1997), Lonsdale et al. (1990), Saunders et al. (1990) and Rowan-Robinson et al. (1990) and at 850  $\mu\text{m}$  from Smail et al. (1997), Hughes et al. (1998), Barger et al. (1999), Blain et al. (1999), Borys et al. (2002), Scott et al. (2002) and Webb et al. (2002).

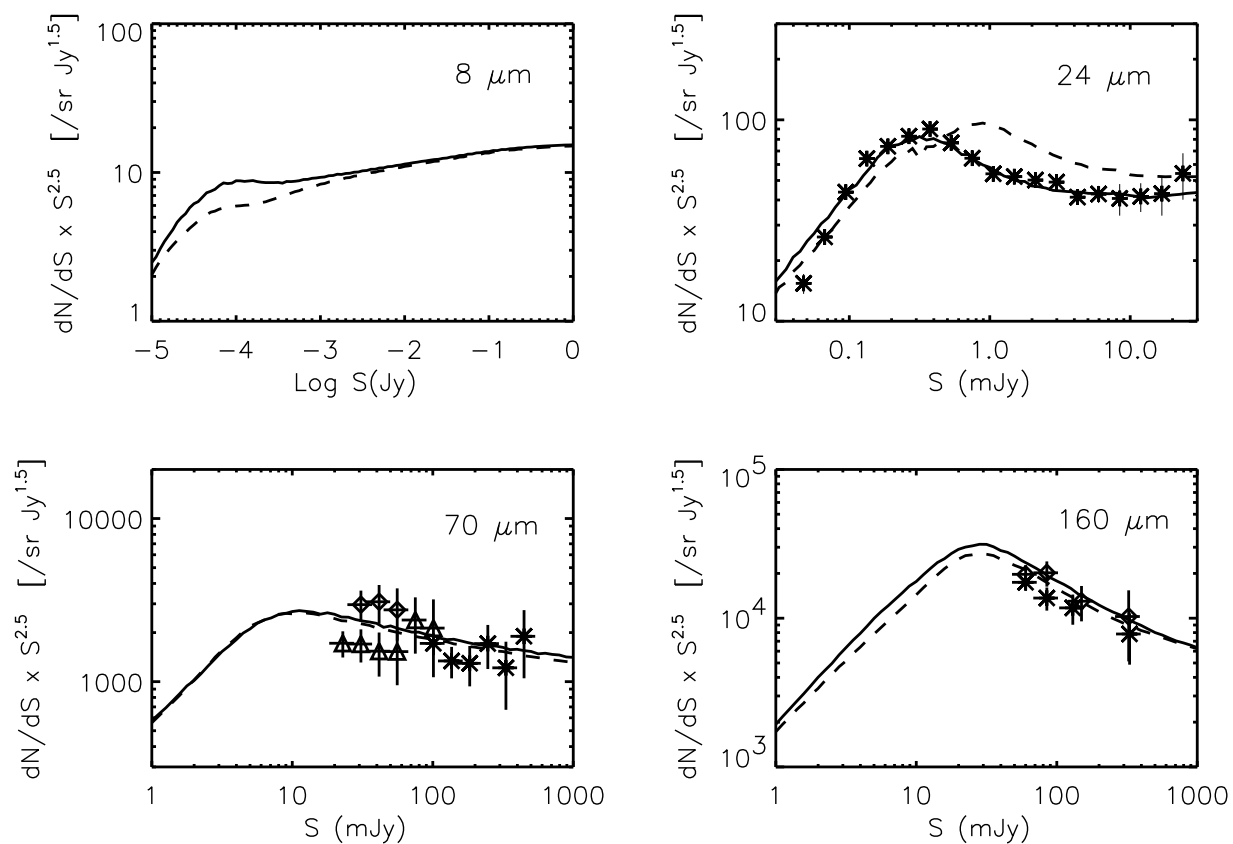


Fig. 4.— Number counts at 24, 70 and 160  $\mu\text{m}$  together with the model predictions (present work: continuous line, Lagache et al. 2003: dashed line). Data at 24, 70 and 160  $\mu\text{m}$  are from Papovich et al. (2004) and Dole et al. (2004a). Notice that none of the observed source counts are corrected for incompleteness.

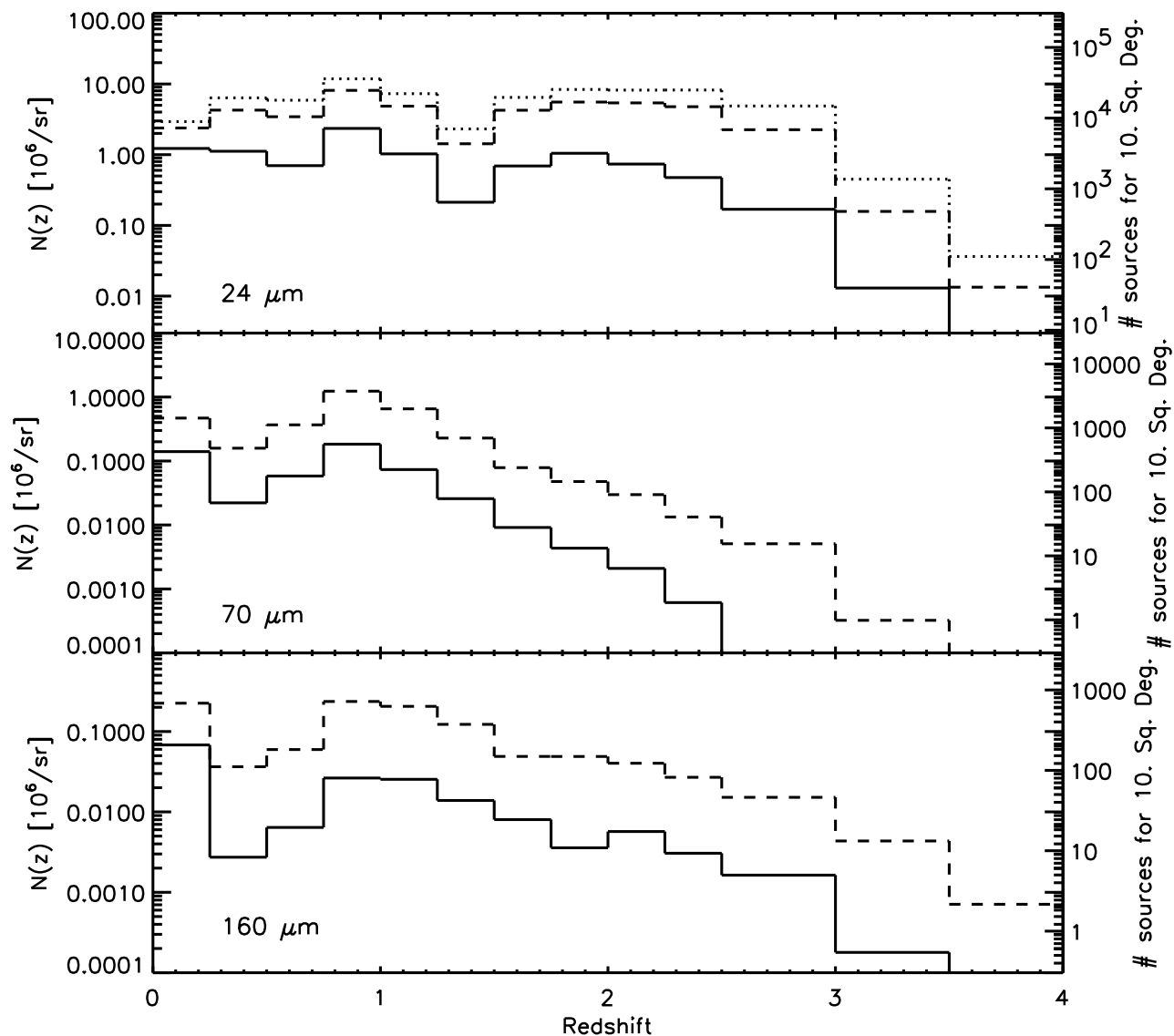


Fig. 5.— MIPS 24, 70 and 160  $\mu\text{m}$  redshift distributions (in logarithmic scale). *Solid lines*: Shallow surveys (flux greater than 0.3, 22.3 and 135.1 mJy at 24, 70 and 160  $\mu\text{m}$  respectively), *dashed line*: Deep surveys (flux greater than 0.094, 6.8, 50.2 mJy at 24, 70 and 160  $\mu\text{m}$  respectively), *Dotted line*: Ultra Deep survey (flux greater than 0.06 mJy at 24  $\mu\text{m}$ ).

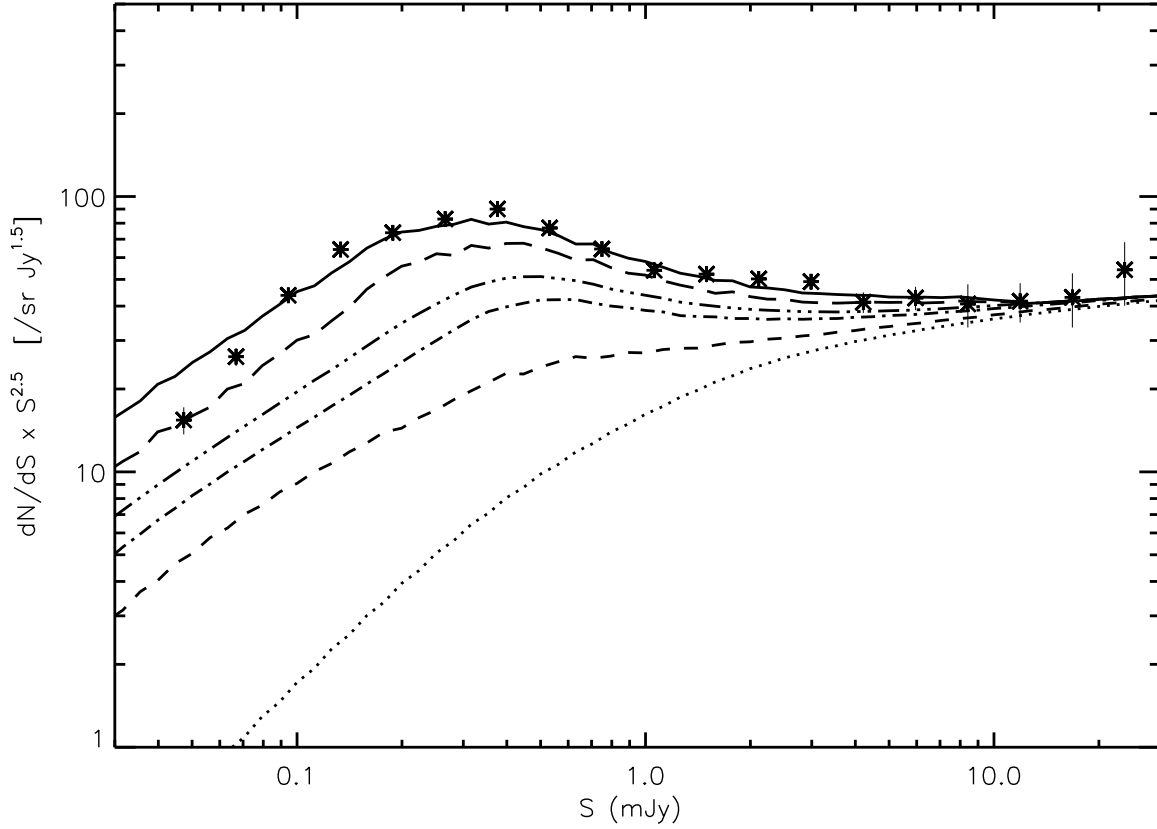


Fig. 6.— Redshift contribution to the number counts at  $24 \mu\text{m}$ . The dot, dash, dash-dot, dash-3 dot, long-dash correspond to the number counts up to redshifts 0.3, 0.8, 1, 1.3 and 2 respectively. Data are from Papovich et al. (2004).

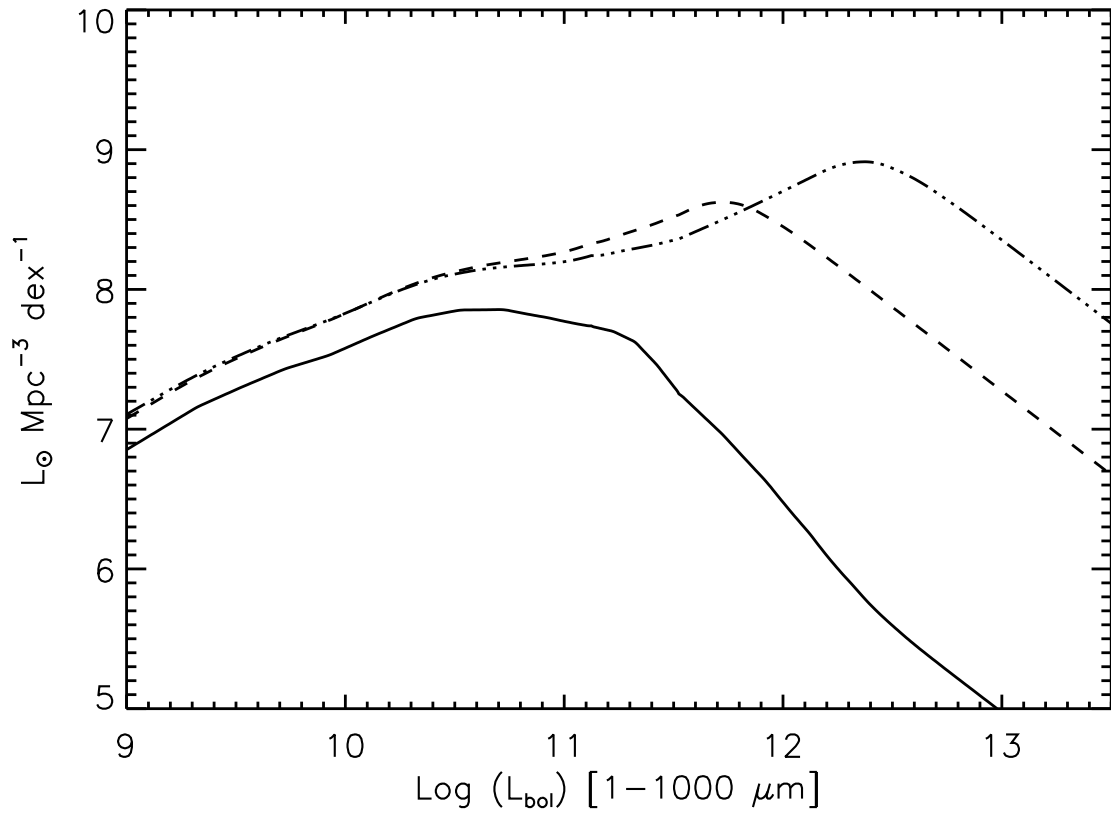


Fig. 7.— Co-moving evolution of the IR energy output per dex of luminosity ( $L \text{ dN}/\text{dLogL}$ ). The continuous, dashed, dashed-3dotted lines are for  $z=0, 0.5$  and  $2$  respectively.